Article:
Stewart, D.I., Tay, Y.Y. and Cousens, T.W. (2001) The strength of unsaturated bentonite-enhanced sand. Geotechnique, 51 (9). pp. 767-775. ISSN 0016-8505

https://doi.org/10.1680/geot.51.9.767.41034

Stewart, D. I., Tay, Y. Y. & Cousens, T. W. (2001). *Géotechnique* **51**, No. 9, 767–775

The strength of unsaturated bentonite-enhanced sand

D. I. STEWART*, Y. Y. TAY* and T. W. COUSENS*

A modification to Rowe's stress-dilatancy equation is presented that extends its range of application to include unsaturated soil behaviour. The results of a programme of constant water content triaxial tests on unsaturated bentonite-enhanced sand (BES) are reported, together with those of a programme of saturated drained triaxial tests on the sand. It is shown that the variation in the rate of dilation at failure with the sand relative density is similar for the two materials. It is proposed that the packing and friction angle of the sand particles and the degree of saturation control the shear strength of unsaturated BES containing modest amounts of bentonite, and that the shear strength of the bentonite component can be ignored.

KEYWORDS: cut-off walls and barriers; friction; laboratory tests; partial saturation; shear strength; suction.

Nous présentons une modification de l'équation de Rowe portant sur la contrainte-dilatance. Elle étend son domaine d'application au comportement des sols non saturés. Nous rapportons les résultats d'un programme d'essais triaxiaux sur la teneur en eau constante d'un sable non saturé amélioré par de la bentonite (BES) ainsi que les résultats d'un programme d'essais triaxiaux saturés et drainés sur le sable. Nous montrons qu'une variation du taux de dilatation au point de rupture avec la densité relative du sable est similaire pour les deux matériaux. Nous avançons que le compactage et l'angle de friction des particules de sable et le degré de saturation contrôlent la résistance au cisaillement du sable BES non saturé contenant de modestes quantités de bentonite et que la résistance au cisaillement du composant bentonite est négligeable.

INTRODUCTION

Bentonite-enhanced sand (BES) is often used to form low hydraulic conductivity barriers to minimise the leakage of contaminated liquids from landfills and other waste containment facilities. While low hydraulic conductivity is often the primary design consideration, landfill liners should also have sufficient strength for stability during construction and operation.

The degree of saturation of BES after compaction is unlikely to exceed about 90% and, where the BES liner is protected from rainfall, it is unlikely that full saturation will be achieved prior to landfilling. Indeed, the saturation of a BES layer in a composite liner may decrease after construction if a primary HDPE (high-density polyethylene) liner is employed. Therefore the rational design of BES liners to avoid slope stability and bearing capacity failures should be based on unsaturated strength parameters if it is to avoid undue conservatism.

This paper presents a modification to the stress-dilatancy equation of Rowe (1962) to describe unsaturated soil behaviour. It reports strength data from constant moisture content, axis-translation, and triaxial compression tests on unsaturated BES. It is shown that interactions between the sand particles control the strength of unsaturated BES containing modest amounts of bentonite. Finally, a rational approach to interpreting unsaturated strength data from BES specimens compacted over a range of moisture contents to different dry densities is proposed.

BACKGROUND

Unsaturated soil mechanics first emerged as a distinct discipline in the late 1950s. At that time several authors proposed similar modifications of Terzaghi's principle of effective stress to cover unsaturated soils (see Bishop, 1960a, b). The expression proposed by Bishop has now become the most widely adopted because it covers the situation where both the pore air and pore water pressures are non-zero. Bishop's equation can be written

$$\sigma' = (\sigma - u_a) + \chi(u_a - u_w) \quad (1)$$

where σ' is the effective normal stress, σ the total normal stress, u_a the pore air pressure and u_w the pore water pressure.

Manuscript received 26 October 2000, revised manuscript accepted 5 July 2001.
Discussion on this paper closes 1 May 2002, for further details see inside back cover.
* University of Leeds, School of Civil Engineering, Leeds.

In this paper the terms $(\sigma - u_a)$ and $(u_a - u_w)$ are described as the net normal stress, σ'', and suction, s. The parameter χ describes the impact of suction on the effective normal stress. The value of χ depends primarily on the degree of saturation, but is also influenced by factors such as soil structure, the cycle of wetting and drying and stress change (Bishop, 1960a). Equation (1) is most usually combined with the Mohr–Coulomb strength equation to describe soil strength. For frictional soil this yields the Mohr's circle diagram for failure shown in Fig. 1. Using this approach the principal stresses at failure are given by

$$\sigma_1'' = \sigma_3'' \tan^2(45° + \phi/2) + \chi s[\tan^2(45° + \phi/2) - 1] \quad (2)$$

where ϕ is the drained angle of shearing resistance of the soil.

The effective stress approach to unsaturated soil behaviour makes the implicit assumption that the soil's response to an effective stress change does not depend on whether that change is due to an increment of net stress, suction or a combination of the two. However, it has been shown that the effective stress approach cannot explain the volumetric behaviour of unsaturated soils subjected to different combinations of net stress and suction. As a result, net stress and suction are treated as independent stress state variables (see for example Jennings & Burland, 1962; Matyas & Radhakrishna, 1968; Fredlund & Morgenstern, 1977), with the benefit that the stress variables are then independent of saturation and all other material properties.

Fredlund *et al.* (1978) proposed the following shear strength equation based on the independent stress state variables of net normal stress and suction:

$$\tau_f = c' + \sigma'' \tan\phi + s \tan\phi^b \quad (3)$$

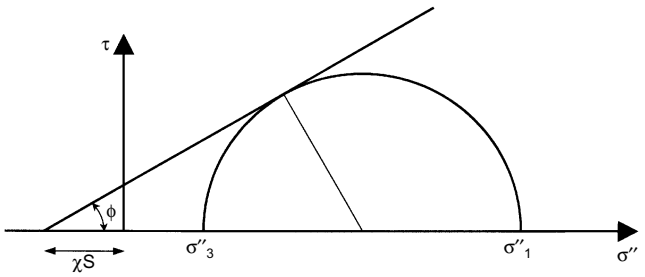

Fig. 1. Mohr's circle at failure for an unsaturated cohesionless soil obeying the modified principle of effective stress

where c' is the effective cohesion and ϕ^b is the angle of internal friction with respect to suction. Thus in a cohesionless soil at failure the principal stresses are given by

$$\sigma_1'' = \sigma_3'' \tan^2(45° + \phi/2) + s\frac{\tan\phi^b}{\tan\phi}[\tan^2(45° + \phi/2) - 1] \quad (4)$$

Equations (3) and (4) describe the same strength envelope when $\tan\phi^b = \chi\tan\phi$.

More recently there has been significant progress in describing the stress–strain behaviour of unsaturated fine-grained soil within a critical-state framework (e.g. Alonso *et al.*, 1990; Toll, 1990; Wheeler & Sivakumar, 1995). Notably, Alonso *et al.* (1990) proposed an elasto-plastic work-hardening constitutive model for unsaturated soils based on the stress variables of the mean net stress and suction. It assumes a yield surface that defines when plastic strains will occur, which on constant-s planes is equivalent to the modified cam-clay yield locus. Within the model three parameters define the size of the yield surface at a particular stress state, and thereby describe strength. These are the conventional critical-state friction parameter, M, a parameter, k, that determines the variation of tensile strength with suction (i.e. one intercept of the yield surface with the $q = 0$ plane), and the preconsolidation pressure (whose locus in the $q = 0$ planes is termed the loading collapse yield curve).

None of the current unsaturated soil models is without problems. Owing to its relative simplicity the effective stress approach is still widely used by practitioners to estimate the shear strength of unsaturated soil. However, a serious shortcoming of the approach is that χ cannot be determined from other soil properties such as saturation, and attempts to quantify χ using simple capillary models to evaluate the effect of suction on the interparticle stress have met with little success (Khalili & Khabbaz, 1998). The independent state variable approach of Fredlund & Morganstern (1977) rationalises the choice of stress variables, but ϕ^b varies non-linearly with suction, and has not been successfully related to either the degree of saturation of the soil or the fundamental friction properties of the soil particles. Therefore the predictive capacity of both approaches is limited to situations where either χ or ϕ^b has been established experimentally over the relevant range of suction.

The elasto-plastic constitutive models of Alonso *et al.* (1990), and others, have much to recommend them, particularly because they can model the important features of unsaturated soil behaviour (e.g. the increase of strength and stiffness changes with suction and the possibility of collapse on wetting) within a single rational framework. However, the relationships between shear strength and suction that are assumed within these models have yet to be related to the fundamental friction properties of the soil particles, and owing to their complexity such models are primarily research tools at present.

This paper proposes that the shear strength of unsaturated soil is related to the forces between the particles, the packing of these particles and the interparticle friction (as for saturated soils), and thus the strength equation should contain a single friction parameter.

Rowe's stress-dilatancy theory applied to unsaturated soil

Rowe (1962) considered the behaviour of idealised, regularly packed systems analogous to cohesionless soil, and developed an equation that relates the effective stress ratio to the surface friction, ϕ_μ, and the rate of dilatancy:

$$\frac{\sigma_1'}{\sigma_3'} = \tan^2(45° + \phi_\mu/2)\left(1 - \frac{\dot\varepsilon_v}{\dot\varepsilon_1}\right) \quad (5)$$

where $\dot\varepsilon_v$ and $\dot\varepsilon_1$ are the volumetric and major principal strain rates (compression positive). Rowe then demonstrated experimentally that a similar equation describes the stress-dilatancy behaviour of both coarse and fine sands. However, Rowe (1962) acknowledged that equation (5) tends to underestimate the strength of random materials when there is significant particle reorientation during shearing. Rowe proposed that the parameter ϕ_f should replace ϕ_μ in equation (5), and suggested that $\phi_f \approx \phi_{crit}$ for loose materials where failure is associated with turbulent shear, but $\phi_f \approx \phi_\mu$ for denser materials where particle sliding is dominant at failure. Thus, at failure, equation (5) becomes

$$\left(\frac{\sigma_1'}{\sigma_3'}\right)_f = \tan^2(45° + \phi_f/2)\left(1 - \frac{\dot\varepsilon_v}{\dot\varepsilon_1}\right)_f \quad (6)$$

It has subsequently been shown that Rowe's stress-dilatancy equation can be developed without assuming regular particle packing (De Josselin de Jong, 1976).

One shortcoming of Rowe's stress-dilatancy approach to the shearing of soils is that it ignores particle rolling, and assumes that energy is dissipated only by sliding friction between particles. Horne (1965) and Rowe (1972) argue that sliding within a random assembly of particles occurs only on favourably orientated planes, so that relative motions within the assembly are restricted to those between large groups of particles that move instantaneously relative to each other before reforming into new groups. This favours sliding over rolling as the main mode of interparticle motion. However, Skinner (1969) showed that Rowe's method of directly measuring interparticle friction does not completely eliminate particle rolling and thus, because Rowe (1962) reports good agreement between the ϕ_μ values derived from triaxial data for denser materials and those from direct measurements, some particle rolling must occur even when packing is dense. Despite some reservations about the physical interpretation of ϕ_f, stress-dilatancy theory is used in this paper because it is amenable to the inclusion of capillary forces since it considers the force equilibrium at particle contacts, and thus, as a minimum, should provide a means of gaining useful insight into unsaturated soil strength.

Figure 2(a) is a plan view of an array of uniform spheres in face-centred cubic packing. Fig. 2(b) is a view of plane X–X. In plane X–X the external spheres are subjected to vertical and horizontal forces L_1 and L_3 due to the applied stresses σ_1'' and σ_3''. Owing to symmetry the forces between two spheres in plane X–X can be deduced from equilibrium. These forces are shown in Fig. 2(c), where S is the suction force, which acts normal to the point of contact. If points of contact normal to the plane at an angle β to the principal stress direction are in a state of limiting equilibrium, then

$$L_1 = 2L_3\tan(\beta + \phi_f) + 4S\tan\phi_f\frac{\sec\beta}{(1 - \tan\beta\tan\phi_f)} \quad (7)$$

Substituting $\sigma_1'' = L_1/l_3^2$ and $\sigma_3'' = L_3/l_1 l_3$ (where l_1 and l_3 are the vertical and horizontal spacing of the spheres in plane X–X) and defining α such that $\tan\alpha = 2l_1/l_3$, then

$$\sigma_1'' = \sigma_3''\tan\alpha\tan(\beta + \phi_f) + \frac{2\,S\tan\phi_f}{l_1 l_3}\frac{\tan\alpha\sec\beta}{(1 - \tan\beta\tan\phi_f)} \quad (8)$$

Expressing the interparticle force due to suction as a stress by dividing it by the cross-sectional area in plane β associated with a single contact ($= l_1 l_3/2\cos\beta$), and assuming that this stress is a fraction, χ^*, of the suction, s, then

$$\sigma_1'' = \sigma_3''\tan\alpha\tan(\beta + \phi_f) + \chi^* s\tan\phi_f\frac{\tan\alpha\sec^2\beta}{(1 - \tan\beta\tan\phi_f)} \quad (9)$$

Figure 3 shows the relative movements of four neighbouring spheres in plane X–X. If deformation of the array causes β, the angle of the tangent at the point of contact, to decrease by a small amount $\Delta\beta$, then

$$\frac{\delta_1}{2} = d\sin\beta - d\sin(\beta - \Delta\beta) \quad \text{and}$$

$$\frac{\delta_3}{2} = d\cos(\beta - \Delta\beta) - d\cos\beta \quad (10)$$

where d is the sphere diameter, and $\delta_1/2$ and $\delta_3/2$ are the

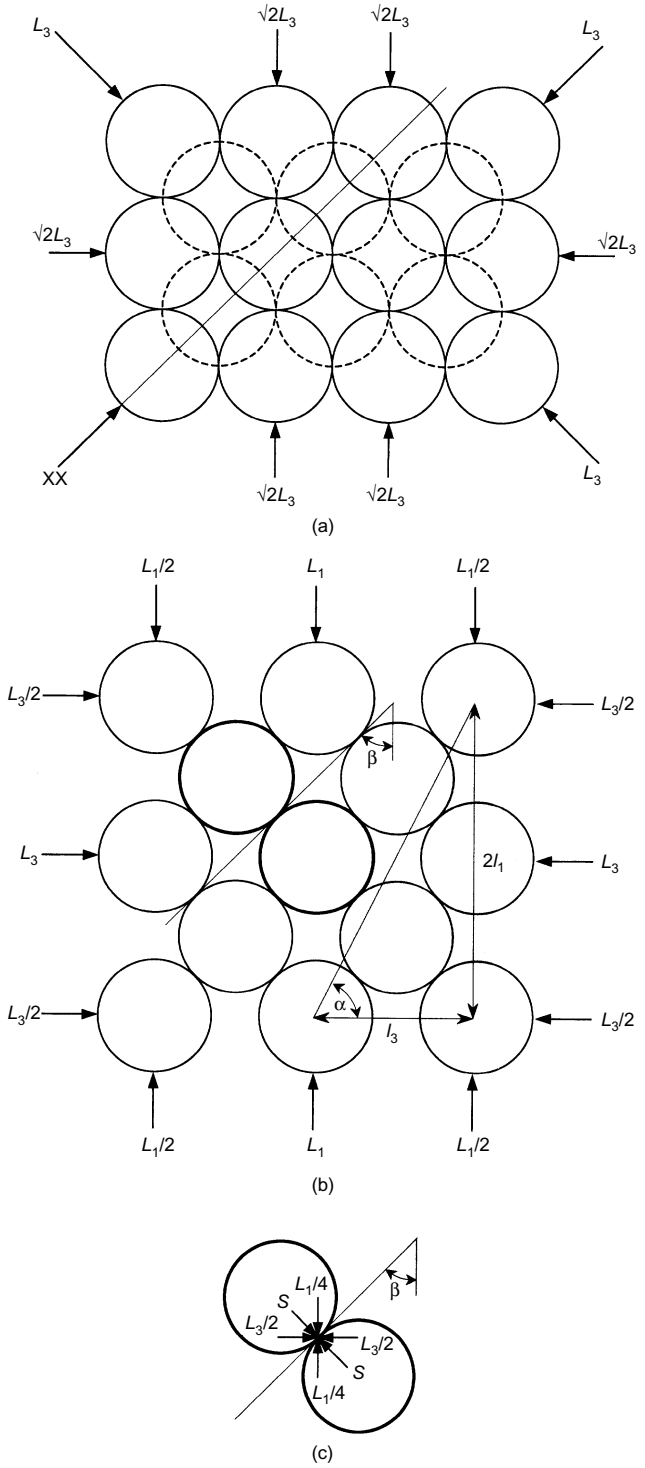

Fig. 2. Uniform spheres in face-centred-cubic packing: (a) plan; (b) plane X–X; (c) forces at a point of contact (after Rowe, 1962)

relative displacements of spheres in sliding contact in the vertical and horizontal directions. When $\Delta\beta$ is small, the ratio of instantaneous deflection increments is

$$\frac{\dot{\delta}_3}{\dot{\delta}_1} = \tan\beta \tag{11}$$

and the ratio of instantaneous strain increments is:

$$\frac{\dot{\varepsilon}_3}{\dot{\varepsilon}_1} = \frac{l_1}{l_3}\frac{\dot{\delta}_3}{\dot{\delta}_1} = \frac{-1}{2}\tan\alpha\tan\beta \tag{12}$$

During deformation work is done by the major principal stress, and work is done against both the minor principal stress and the suction (spheres in the same horizontal plane tend to separate, and if capillary water initially bridges between these spheres, net work is done against the suction stress). Thus for unsaturated soil Rowe's energy ratio is

$$\dot{E} = \frac{\sigma_1''\dot{\varepsilon}_1}{-2(\sigma_3'' + \chi^* s)\dot{\varepsilon}_3} = \frac{\sigma_3''}{(\sigma_3'' + \chi^* s)}\frac{\tan(\beta + \phi_f)}{\tan\beta} + \frac{\chi^* s}{(\sigma_3'' + \chi^* s)}\frac{2\tan\phi_f}{\sin 2\beta(1 - \tan\beta\tan\phi_f)} \tag{13}$$

If the particle array deforms so as to absorb a minimum amount of internal work in frictional heat for any given stress state, then β for this condition is given by $d\dot{E}/d\beta = 0$. The differentials of both terms in equation (13) come independently to zero when $\beta = (45° - \phi_f/2)$. Substituting this value into equation (13) and noting that volume compatibility yields

$$\frac{-2\dot{\varepsilon}_3}{\dot{\varepsilon}_1} = \left(1 - \frac{\dot{\varepsilon}_v}{\dot{\varepsilon}_1}\right) = D:$$

$$\sigma_1'' = \sigma_3''\tan^2(45° + \phi_f/2)D + 2\chi^* s\tan\phi_f\tan(45 + \phi_f/2)D \tag{14}$$

This result is essentially the same as that proposed by Rowe *et al.* (1963) for soil with both friction and cohesion, where $\chi^* s\tan\phi_f$ is analogous to the cohesive component of strength.

Rearranging equation (14) gives

$$\sigma_1'' = \sigma_3''\tan^2(45° + \phi_f/2)D + \chi^* s\,D[\tan^2(45° + \phi_f/2) - 1] \tag{15}$$

Thus the strength component due to net stress is a function of the conventionally defined drained angle of shearing resistance [i.e. $\tan^2(45° + \phi/2) = D\tan^2(45° + \phi_f/2)$], whereas the component due to suction is a more complex function of particle friction, the parameter χ^* and the rate of dilation. Comparison with equation (2) indicates that the parameters χ and χ^* are not equivalent. The proposed parameter χ^* is defined as the ratio of the suction stress to the suction (i.e. it is the parameter that capillary pore water models attempt to evaluate), whereas χ for a particular soil will vary with the rate of dilation at failure. This difference between χ and χ^* may, at least in part, explain the difficulty in obtaining consistent unsaturated strength data from densely packed soils, and why χ values based on capillary theory often differ from those determined from strength data.

MATERIALS

The materials used were SPV 200 Wyoming bentonite supplied by Cetco Europe Ltd (formerly Volclay), and Sherburn yellow building sand supplied by Tom Langton and Sons, Leeds, UK. SPV 200 bentonite originates from Lovell, Wyoming, USA, and is a well-ordered sodium montmorillonite with minor quartz and cristobolite impurities (Studds *et al.*, 1998). Sherburn sand is predominantly a quartz sand (suppliers specification). Other properties of these materials are given in Table 1.

METHODS

BES containing 10% bentonite by dry weight was prepared at various moisture contents by heavy manual compaction (BS1377: Part 4: 1990), and specimens 76 mm × 38 mm in diameter were cored. Triaxial testing was conducted in standard Wykeham Farrance 38 mm triaxial cells equipped with 3 kN submersible load cells, and 'Imperial College type' volume change units measuring the change in cell fluid volume. Prior to testing, the cell was calibrated for apparent volume change due to leakage etc. The cell correction factor was found to be relatively insensitive to cell pressure over the range used in the tests, and a value of $1{\cdot}3 \times 10^{-6}$ ml/s was used. Testing was conducted at 21 ± 1°C, and the accuracy of individual measurements was estimated to be ±1 kPa for pressure, ±1 kPa deviator stress, ±0·005 mm for displacement, and ±0·025 ml for volume change. Hence the accuracy of the axial and volumetric strain measurements is better than ±0·03%. Rates of dilation at failure were estimated by

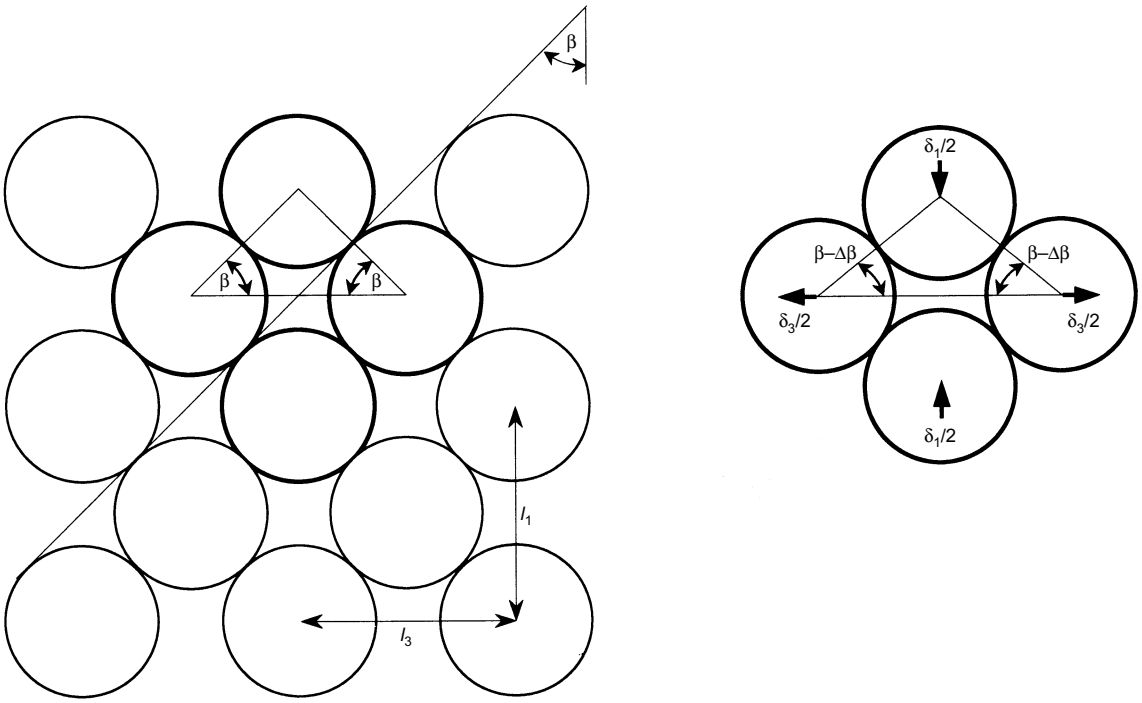

Fig. 3. Relative movement of the spheres in the plane X–X

Table 1. Properties* of SPV200 Wyoming bentonite and Sherburn yellow building sand

SPV200 Wyoming bentonite	Sherburn yellow building sand
Average particle size = 2 μm†	Effective size, D_{10} = 212 μm
Specific gravity = 2·751†	Fines = 0·36%
Liquid limit = 354%†	Coefficient of uniformity = 2
Plastic limit = 27%†	Specific gravity = 2·68
Moisture content = 13% (as supplied)	Max and min void ratio‡ = 0·767, 0·375
	Moisture content ≈ 4% (as supplied)
	Angle of repose§ = 34°

*Tests performed in accordance with BS 1377: Part 2: 1990 unless otherwise indicated.
†Studds *et al.* (1998).
‡Determined by methods described in Head (1980).
§Determined by method recommended by Cornforth (1973).

locally fitting a straight line to the strain data by regression analysis, with an estimated accuracy of better than ±0·03.

Triaxial tests on compacted BES were conducted using the axis-translation technique. Elevated pore air pressure was used to raise the pore water pressure to avoid cavitation in the measurement system. The pore air pressure was supplied to a coarse porous ceramic disc in the pedestal of the triaxial cell. The pore water pressure line was connected to a high air-entry porous ceramic disc mounted in the top cap of the triaxial cell. Standard Araldite epoxy resin (CIBA-Geigy Plastics and Additives Company) was used to seal the ceramic into the acrylic top cap. De-airing of the pore water pressure line was achieved by filling the triaxial cell with de-aired water without a specimen present, and lightly pressurising the cell to induce flow through the pore water line. After several hours of flow the tap in the pore water line was closed and the cell pressure was increased to 800 kPa for 24 h to dissolve any air that remained in the line.

A programme of consolidated constant water content (CW) tests was conducted. Initially the specimens were subjected to a cell pressure equal to the required σ_3'' value. Then the cell and pore air pressures were increased together while maintaining σ_3'' until the pore air pressure reached a value sufficient to induce a positive pore water pressure in the specimens. Next the specimens were allowed to consolidate until the pore water pressure reached equilibrium (which typically took 2 weeks). Finally the specimens were axially compressed at a rate of 0·0004 mm/min until either a peak deviator stress was reached or 20% axial strain was exceeded (the time to failure varied between 9 and 26 days).

In addition to the tests on BES, a series of conventional drained triaxial compression tests were performed on Sherburn sand specimens prepared dry at various void ratios by 'sand raining' and then saturated by back-pressure (see Tay, 2000, for details).

RESULTS

Figure 4 shows the heavy manual compaction curve for BES. The maximum dry density is about 2010 kg/m^3 at an optimum moisture content of about 9·5%. Table 2 presents the results from the CW axis-translation triaxial tests on unsaturated BES. In the table, failure is being defined as the point where peak deviator stress was mobilised. Volumetric strains during consolidation were typically about 4%. However, the initial density of the triaxial specimens (i.e. after consolidation) was about 2·5% lower than that achieved during compaction owing to disturbance during coring.

Table 3 presents the results of the drained triaxial tests on Sherburn sand. As the relative density $[I_D = (e_{max} - e)/(e_{max} - e_{min})]$ increased from about 0·1 to 0·55, ϕ (the maximum angle of shearing resistance) increased from just under

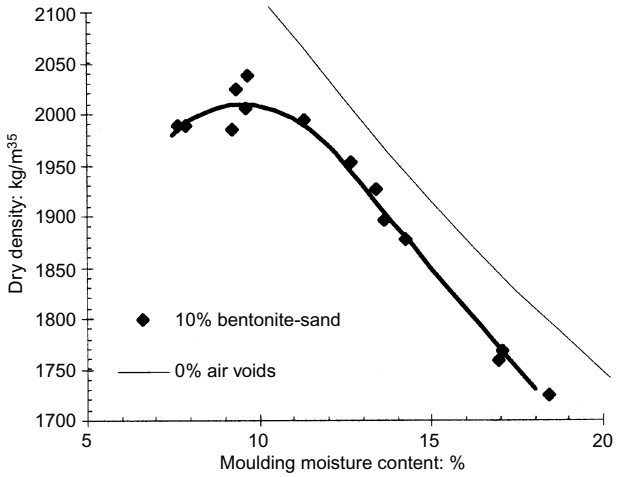

Fig. 4. Compaction curve for BES containing 10% bentonite

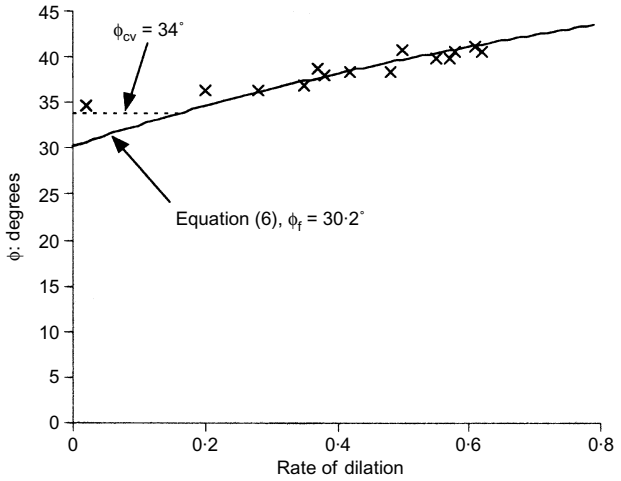

Fig. 5. Variation in the maximum angle of shearing resistance with the rate of dilation for Sherburn yellow building sand

35° to about 41°, with the maximum dilation rate increasing with the initial relative density of the specimen. Fig. 5 shows the variation in the maximum angle of shearing resistance of Sherburn sand with the dilation rate. Also shown in Fig. 5 is the stress-dilatancy equation (6) based on $\phi_f = 30{\cdot}2°$, an average value calculated for the specimens that exhibited appreciable dilation at failure (i.e. all specimens except 0d11). Rowe (1962) reported a similar value of $\phi_f = 29°$ for fine quartz sand. Specimen 0d11 (the data point furthest to the left in Fig. 5) was very loose, compressed upon shearing, and exhibited very little dilation at failure. For this specimen the estimated ϕ_f value was 34·2°, which is very close to the sand ϕ_{crit} value of 34° (ϕ_{crit} is roughly equal to the angle of repose; Cornforth, 1973).

Figures 6(a) and 6(b) shows the axial and volumetric strain to failure of both saturated sand and unsaturated BES plotted against the sand relative density. For BES, $I_{D,s}$ is defined as the relative density calculated using the sand void ratio, e_s [where e_s = (volume of clay and voids)/(volume of sand)]. Bolton (1986) successfully used relative density to compare sand triaxial data where the mean effective stress varied by a factor of 4, because strength and rate of dilation vary logarithmically with stress and hence the effect of stress on the classification parameter can be ignored for such a stress range. Here it would also be difficult to use a more sophisticated parameter owing to uncertainty about the impact of suction on interparticle stress.

Table 2. Results of the axis-translation CW triaxial tests on unsaturated 10% bentonite–sand mixtures

ID	$(m.c.)_i$: (%)	$(\rho_{dry})_i$: (kg/m^3)	$(I_{D,s})_i$	$(S_r)_i$	σ_3: (kPa)	U_a: (kPa)	$(\sigma_1 - \sigma_3)_f$: (kPa)	$(U_w)_f$: (kPa)	$(\varepsilon_1)_f$: (%)	$(\varepsilon_v)_f$: (%)	$\left(-\frac{\dot{\varepsilon}_v}{\dot{\varepsilon}_1}\right)_f$
10ax5	9·1	1939·4	0·59	0·64	248·0	196·5	599·3	11·8	7·3	−0·51	0·72
10ax8	9·6	1997·0	0·71	0·75	267·0	167·3	738·7	10·9	6·5	−0·41	0·63
10ax2	9·7	1935·6	0·59	0·67	267·0	168·0	735·7	22·4	7·8	−0·42	0·65
10ax4	11·7	1906·4	0·53	0·77	514·0	113·0	1537·0	8·0	8·0	−0·27	0·40
10ax6	12·1	1908·4	0·53	0·80	150·0	100·3	489·3	−0·4	11·8	−0·89	0·54
10ax1	12·3	1898·1	0·51	0·80	230·0	180·1	451·7	94·3	12·0	−2·80	0·52
10ax10	12·6	1888·7	0·49	0·80	564·0	167·5	1355·5	70·9	12·6	−0·62	0·30
10ax9	13·2	1856·4	0·42	0·79	568·5	168·8	1321·8	89·3	16·5	0·02	0·28
10ax7	13·8	1804·7	0·30	0·76	234·0	133·1	441·7	60·8	19·3	1·15	0·26
10ax13	14·0	1798·4	0·29	0·76	553·0	153·2	1282·0	64·5	20·0	0·94	0·22
10ax3	14·7	1724·2	0·11	0·71	218·0	118·3	407·2	49·9	20·0	1·18	0·10

Note: The subscripts i and f indicate the initial and failure values, respectively.

Table 3. Results of the drained triaxial tests on saturated Sherburn yellow building sand

ID	$(\rho_{dry})_i$: (kg/m^3)	$(I_D)_i$	σ_3: (kPa)	u: (kPa)	$(\sigma_1 - \sigma_3)_f$: (kPa)	$(\varepsilon_1)_f$: (%)	$(\varepsilon_v)_f$: (%)	$\left(-\frac{\dot{\varepsilon}_v}{\dot{\varepsilon}_1}\right)_f$	ϕ: (°)
0d11	1539·6	0·07	399·4	300·0	263·2	14·7	0·77	0·02	34·7
0d13	1633·4	0·33	400·3	300·0	290·4	10·4	−1·24	0·28	36·3
0d5	1640·1	0·34	360·0	300·0	191·6	10·7	−1·77	0·38	37·9
0d7	1646·2	0·36	353·2	300·0	173·8	9·0	−1·65	0·42	38·3
0d16	1650·4	0·37	500·6	300·0	581·9	9·7	−1·08	0·20	36·3
0d3	1664·6	0·40	353·2	300·0	177·5	10·1	−1·55	0·37	38·7
0d12	1674·6	0·43	400·2	300·0	329·6	8·4	−1·80	0·48	38·4
0d14	1696·5	0·48	500·2	300·0	598·1	7·8	−0·89	0·35	36·8
0d6	1710·9	0·56	353·4	300·0	191·2	8·2	−1·86	0·55	39·9
0d4	1712·6	0·52	358·5	300·0	218·2	7·3	−1·39	0·58	40·6
0d9	1717·6	0·53	350·1	300·0	188·2	8·5	−1·52	0·50	40·7
0d1	1734·2	0·54	349·9	300·0	192·4	7·2	−1·20	0·61	41·2
0d8	1723·2	0·54	353·6	300·0	199·3	8·4	−2·35	0·62	40·6
0d15	1728·6	0·56	402·0	300·0	363·0	7·8	−1·83	0·57	39·8

Note: The subscripts i and f indicate initial and failure values, respectively.

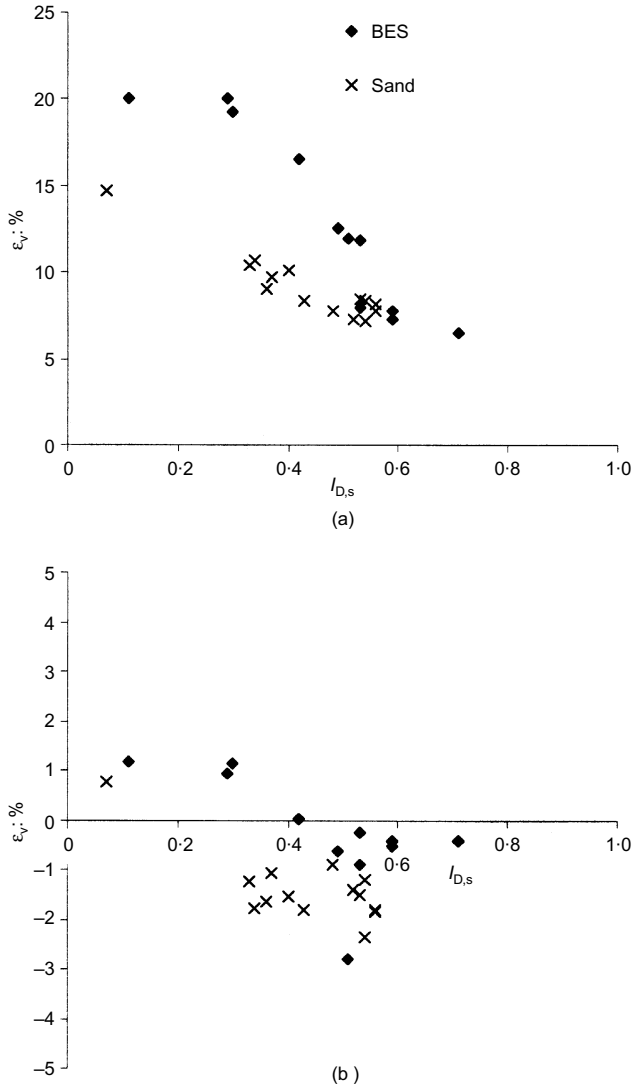

Fig. 6. Variation in strain to failure with sand relative density: (a) axial strain; (b) volumetric strain

For saturated sand, the axial strain to failure decreased from 15% to about 7% as the relative density increased from about 0·1 to about 0·6, and volumetric strain was moderately expansive for all but the loosest specimen, 0d11, which compressed prior to failure. The axial and volumetric strain to failure of unsaturated BES show similar trends to those of saturated sand, but at low $I_{D,s}$ the BES exhibited greater axial strain to failure than the sand, and the overall volumetric strain to failure was compressive for $I_{D,s}$ less than about 0·4 (although all specimens dilated at failure). The volume change of one specimen (10ax1) does not fit the pattern of the other BES data, and neither does it show the same behaviour as specimen 10ax6 (where specimen preparation and test conditions were similar; see Table 2), which may indicate an error in the volume change measurement for this test. From comparing the sand and BES data shown in Fig. 6 it can be inferred that at high $I_{D,s}$ sand particle interactions control the pre-failure deformation of BES, whereas at low $I_{D,s}$ the larger axial strains may indicate that there was initially bentonite gel, which is easily displaced upon loading, separating some sand grains.

Figure 7 shows the rate of dilation at failure of both saturated sand and unsaturated BES plotted against the sand relative density (the line shown on this figure will be discussed later). Fig. 7 shows that BES behaves in a similar manner to sand, and thus it is deduced that sand particle interactions dominate the behaviour of BES at failure.

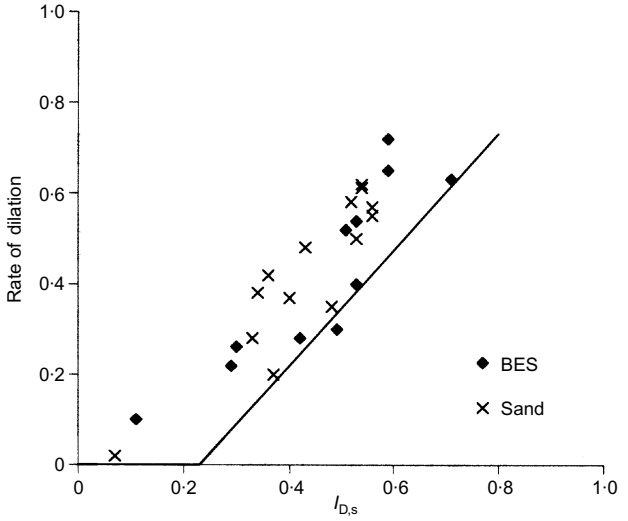

Fig. 7. Variation in rate of dilation at failure with sand relative density

INTERPRETATION

The sand void ratios of the BES specimens were all between the maximum and minimum void ratios for the sand alone, and it has been suggested that their rate of dilation at failure was controlled by sand particle interactions. Thus it is reasonable to assume that there is a matrix of contiguous sand particles within such mixtures. Mollins *et al.* (1999) showed that the peak strength and maximum rate of dilation of saturated BES varied with the sand void ratio in a manner indistinguishable from the behaviour of the sand alone. They concluded that in saturated mixtures containing 5 and 10% bentonite the applied stresses must be supported primarily by a matrix of contiguous sand particles, and that the bentonite made a negligible contribution directly to strength. Thus the strength of such mixtures is governed primarily by the packing of, and friction between, the sand particles.

If it is assumed that the sand matrix supports the applied stresses, and that the bentonite strength can be neglected, then values for the parameter χ^* can be estimated using equation (15). Suitable ϕ_f values were estimated from the sand data presented in Fig. 5 ($\phi_f = 30{\cdot}2°$ for all specimens except 10ax3, which was rather loose and dilated very weakly, where $\phi_f = 32{\cdot}5°$). The estimated χ^* values are shown in Fig. 8 plotted against specimen saturation at failure (estimated from the initial saturation and volumetric strain). The datum point from test 10ax1 is represented by an open symbol as it is considered unreliable, probably underestimating saturation.

Figure 8 shows that at high degrees of saturation ($S_r \approx 0{\cdot}8$) χ^* is close to unity. However, as the degree of saturation decreases below about 0·8 the parameter χ^* decreases rapidly, to about 0·6 when $S_r = 0{\cdot}6$. Over this range, Fig. 8 shows a clear trend between the final degree of saturation and χ^*, with only moderate scatter consistent with experimental variability.

DISCUSSION

Bentonite can absorb many times its own weight of water, and thus it is assumed that all the pore water in BES is associated with the bentonite. Therefore the bentonite in the specimens tested would have formed a gel phase with a moisture content of between 90 and 150%, and would have very little shear strength. It was observed when mixing the BES constituents (prior to compaction) that the bentonite gel tends to coat the sand particles. Compaction then brings the sand grains into close contact. When there is ample water during compaction, there is sufficient bentonite gel to fill most of the pore space in the sand matrix. Trapped air will tend to be surrounded by bentonite gel and therefore isolated from the sand matrix

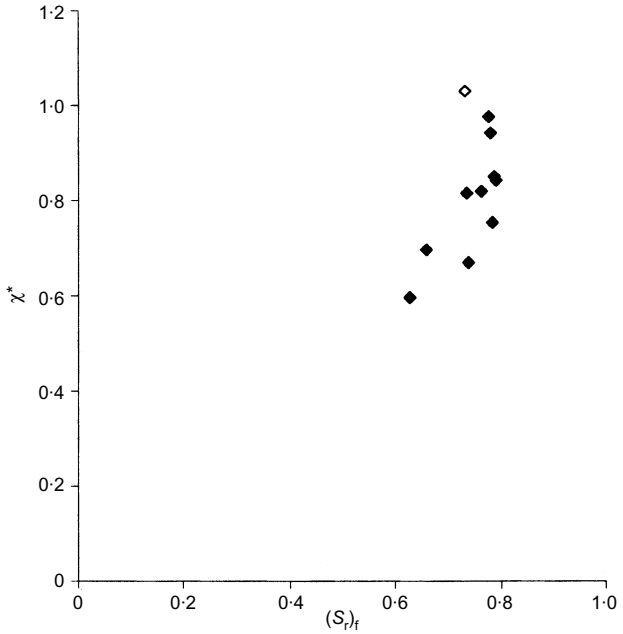

Fig. 8. Estimated χ^* for compacted BES

(see Fig. 9(a)). At lower moisture contents, the volume of the swollen bentonite is smaller, and it coats the sand particles more thinly. After compaction the bentonite will occupy a smaller proportion of the sand pores, and it is suggested that the void air will be less isolated. Such a structure (Fig. 9(b)) is similar to the clay bridging mechanism suggested by Dineen *et al.* (1999).

This proposed structure is compatible with the data in Fig. 8. At high degrees of saturation any air present would be in small pockets isolated from the sand matrix, and thus χ^* would be approximately unity. At lower degrees of saturation, the air trapped during compaction will be less isolated (both from neighbouring pores and the sand matrix), and χ^* would decrease with saturation. In compacted BES it is always likely that a proportion of the bentonite will be relatively distant from the sand particle contacts (unlike free pore water in an unsaturated soil, which tends to be drawn to the particle contacts by capillary action). Thus water in the bentonite gel will be less effective at converting suction into interparticle stress than an equivalent amount of free pore water, and χ^* will decrease rapidly with decreasing saturation.

The data in Fig. 8 showing the dependence of χ^* on S_r were determined for mixtures compacted at various moisture contents to different densities, and then tested without change in moisture content. Despite the different compaction conditions, there is a clear trend between χ^* and S_r. Donald (1960) used a capillary model to show that the parameter called χ^* in this paper depends primarily on saturation, and is relatively insensitive to soil density. Thus it is suggested that, for engineering purposes, the trend between χ^* and S_r shown in Fig. 8 can be treated as a property of the mixture investigated, for any compaction conditions that produce a similar soil structure.

A significant advantage of the stress-dilatancy approach to interpreting unsaturated strength data is that the amount of testing needed to establish the unsaturated strength envelope for a particular soil is greatly reduced. The parameter ϕ_f is a function of soil mineralogy and can be determined in a single saturated drained strength test. Thus each subsequent unsaturated strength test will give χ^* directly if the rate of dilation is measured.

However, the principal advantage of the proposed approach is that equation (15) relates the difference in the principal net stresses at failure to the interparticle friction, rate of dilation, and interparticle stress resulting from suction. These are more fundamental properties of the soil system than are the conventionally used strength parameters (ϕ and either χ or ϕ^b). Thus the strength parameters established using equation (15) should be able to describe the strength of unsaturated soil over a greater range of applied stress and density than is possible using a conventional approach. Indeed, this paper demonstrates that equation (15) can be used to determine a single set of strength parameters for the BES specimens compacted over a range of moisture contents and densities, and which exhibited a significant variation in their rate of dilation at failure (from 0·10 to 0·72). These rates of dilation at failure are equivalent to the drained angle of shearing resistance varying from 34 to 43°. Yet, remarkably, the calculated χ^* values show only modest scatter, and are compatible with a single $\chi^* - S_r$ relationship for the soil.

To use equation (15) predictively, it is necessary to estimate the rate of dilation at failure. This can be found by interpolation from the test data used to establish the strength parameters (e.g. Fig. 7), provided that the data cover the stress range relevant to the intended application. Alternatively, it can be estimated from an empirical correlation with sand relative density and mean effective stress. For example, Bolton (1986) proposed a relative dilatancy index, I_R, that can be correlated with the rate of dilation at failure:

$$I_R = I_D(Q - \ln p') - 1 \tag{16}$$

where p' is in kilopascals. The parameter Q relates to the mean effective stress required to suppress dilatancy, and is related to the crushing strength of the particles (McDowell & Bolton, 1998). Bolton found that $Q = 10$ characterised the behaviour of many quartz and feldspar sands. To estimate the rate of dilation, Bolton proposed the relationship

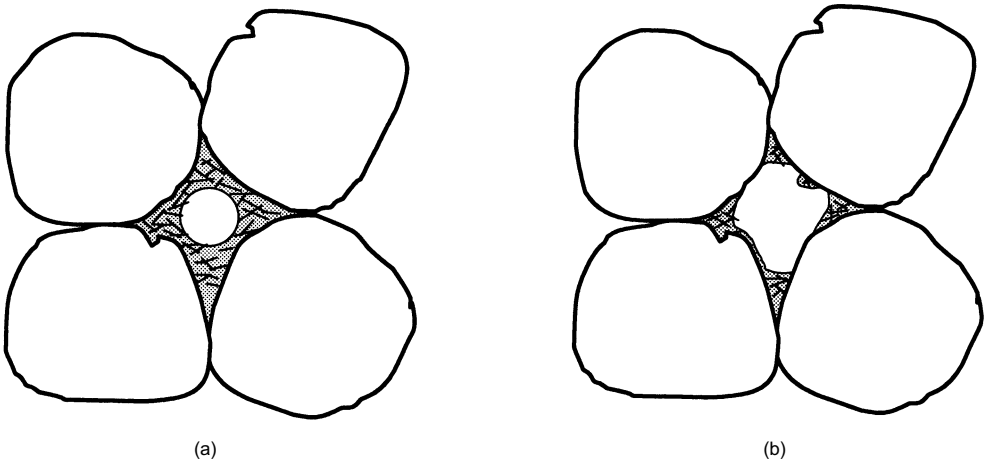

Fig. 9. Idealised structure of BES containing modest amount of bentonite: (a) at high degree of saturation; (b) at intermediate degree of saturation

$$\left(-\frac{\dot{\varepsilon}_v}{\dot{\varepsilon}_1}\right)_{max} = 0{\cdot}3 I_R \quad (17)$$

Equation (17) was used to calculate the position of the line in Fig. 7 using $p' = 300$ kPa (representative of the mean effective/net stress at failure, which ranged from 100 to 900 kPa). A single value was used, owing to the low sensitivity of I_R to p'. Equation (17) slightly underpredicts the rate of dilation of the BES specimens, probably because it overestimates the importance of particle crushing over the stress range investigated (Bolton reports that Karlsruhr sand, which has a similar D_{10} and coefficient of uniformity, behaved similarly). Such an underprediction will produce a safe estimate of unsaturated strength.

Finally, the test data reported in this paper are for mixtures containing 10% bentonite, prepared by heavy manual compaction at moisture contents between optimum and 5% wet of optimum. To apply equation (15) to such mixtures it was assumed that unsaturated strength is controlled by friction and interlocking between the sand particles. This will be appropriate only if the sand relative density is greater than zero and if the bentonite has negligible strength and no impact on the dilatancy of the mixture. It would therefore be unwise to extend this interpretation to mixtures containing significantly more bentonite, or compacted at substantially different moisture contents. However, BES used for landfill liners typically contains around 10% bentonite, and is compacted at a moisture content slightly wet of optimum.

CONCLUSIONS

Rowe's stress-dilatancy equation has been extended to unsaturated soil. This equation indicates that the shear strength due to net stress is proportional to the conventionally defined drained angle of shearing resistance. However, the shear strength due to suction is proportional to the suction-induced stress and a function of particle friction and rate of dilation, and that function will usually be less than the conventionally defined drained angle of shearing resistance. Thus the parameter χ used in the effective stress approach to unsaturated soil strength not only depends on the impact of suction on interparticle stress (as originally envisaged), but will also vary with the rate of dilation at failure.

The dilatancy behaviour at failure of unsaturated compacted BES mixtures typical of those used as landfill liners varies with the sand relative density in a manner that is indistinguishable from the behaviour of sand. It is therefore proposed that frictional interactions between the sand particles control the unsaturated strength of such BES mixtures, and that the strength of the bentonite can be neglected. A stress-dilatancy approach using the sand angle of interparticle friction can then produce rational unsaturated strength parameters for such materials.

NOTATION

c'	effective cohesion
d	sphere diameter
δ_1, δ_3	displacements of spheres in sliding contact in the vertical and horizontal directions
D	strain increment ratio $\left(\frac{-2\dot{\varepsilon}_3}{\dot{\varepsilon}_1} = 1 - \frac{\dot{\varepsilon}_v}{\dot{\varepsilon}_1}\right)$
$\dot{E}$	Ratio of instantaneous work done on a sample to that done by the sample
L_1, L_3	vertical and horizontal forces between spheres in a uniform face-centred cubic array due to the applied stresses σ_1'' and σ_3''
l_1, l_3	vertical and horizontal spacing of the spheres in a uniform face-centred cubic array in plane XX
q	deviator shear stress ($\sigma_1 - \sigma_3$)
s	suction ($u_a - u_w$)
S	inter-particle force due to suction
u_a	pore air pressure
u_w	pore water pressure
α	parameter describing the geometry of packing ($\tan\alpha = 2l_1/l_3$)
β	direction of particle movement with reference to the minor principle plane
χ	parameter that describes the effect of suction on overall strength
χ^*	ratio of the inter-particle stress resulting from suction to the suction
ϕ	drained angle of shearing resistance
ϕ^b	angle of internal friction with respect to suction
ϕ_f	Rowe's friction parameter
ϕ_μ	material friction
ε_v	volumetric strain
ε_1, ε_3	axial and radial strains
σ_1, σ_3	total normal stresses
σ_1', σ_3'	effective normal stresses
σ_1'', σ_3''	net normal stresses ($\sigma - u_a$)
τ	shear stress

A dot superscript denotes incremental change, an 'i' subscript denotes initial conditions and, with the exception of ϕ_f, an 'f' subscript denotes failure.

REFERENCES

Alonso, E. E., Gens, A. & Josa, A. (1990). A constitutive model for partially saturated soils. *Géotechnique* **40**, No. 3, 405–430.

Bishop, A. W. (1960a). Discussion of session 1: General principles and laboratory measurements. In *Pore pressure and suction in soils*, pp. 63–66. London: Butterworth.

Bishop, A. W. (1960b). The measurement of pore pressure in the triaxial test. In *Pore pressure and suction in soils*, pp. 38–46. London: Butterworth.

Bolton, M. D. (1986). The strength and dilatancy of sands. *Géotechnique* **36**, No. 1, 65–78.

British Standards Institution (1990). BS 1377: *Methods of test for soils for civil engineering purposes*. London: British Standards Institution.

Cornforth, D. H. (1973). *Prediction of the drained strength of sands from relative density measurements*, ASTM Special Technical Publication No. 523, pp. 281–303. Philadelphia: American Society for Testing and Materials.

De Josselin de Jong, G. (1976). Rowe's stress-dilatancy relation based on friction. *Géotechnique* **26**, No. 3, 527–534.

Dineen, K., Colmenares, J. E., Ridley, A. M. & Burland, J. B. (1999). Suction and volume changes of a bentonite-enriched sand. *Proc. Inst. Civ. Engrs, Geotech. Engng* **137**, 197–201.

Donald, I. B. (1960). Discussion of session 1: General principles and laboratory measurements. In *Pore pressure and suction in soils*, pp. 69–70. London: Butterworth.

Fredlund, D. G. & Morganstern, N. R. (1977). Stress state variables for unsaturated soils. *J. Geotech. Engng Div., ASCE* **103**, No. GT5, 447–466.

Fredlund, D. G., Morganstern N. R. & Widger, R. A. (1978). Shear strength of unsaturated soils. *Can. Geotech. J.* **15**, 313–321.

Head, K. H. (1980). *Manual of soil laboratory testing*, Vol. 1. London: Pentech Press.

Horne, M. R. (1965). The behaviour of an assembly of rotund, rigid, cohesionless particles: Part I. *Proc. Roy. Soc. Lond. Ser. A*, **286**, 62–78.

Jennings, J. E. B. & Burland, J. B. (1962). Limitations to the use of effective stresses in partly saturated soil. *Géotechnique* **12**, No. 2, 125–144.

Khalili, N. & Khabbaz, M. H. (1998). A unique relationship for χ for the determination of the shear strength of unsaturated soils. *Géotechnique* **48**, No. 5, 681–687.

Matyas, E. L. & Radhakrishna, H. S. (1968). Volume change characteristics of partially saturated soils. *Géotechnique* **18**, No. 4, 432–448.

McDowell, G. R. & Bolton, M. D. (1998). On the micromechanics of crushable aggregates. *Géotechnique* **48**, No. 1, 667–679.

Mollins, L. H., Stewart, D. I. & Cousens, T. W. (1999). Drained strength of bentonite-enhanced sand. *Géotechnique* **49**, No. 4, 523–528.

Rowe, P. W. (1962). The stress-dilatancy relation for static equilibrium of an assembly of particles in contact. *Proc. Roy. Soc. Lond. Ser. A* **269**, 500–527.

Rowe, P. W. (1972). Theoretical meaning and observed values of deformation parameters for soil. In *Stress–strain behaviour of soils* (ed. R. G. H. Parry) , pp. 143–194. London: Foulis.

Rowe, P. W., Oates, D. B. & Skermer, N. A. (1963). The stress-dilatancy performance of two clays. In *Laboratory shear testing of soils*, ASTM Special Technical Publication No. 361, pp. 134–143. Philadelphia: American Society for Testing and Materials.

Skinner, A. E. (1969). A note on the influence of interparticle friction on the shearing strength of a random assembly of spherical particles. *Géotechnique* **19**, No. 2, 150–157.

Studds, P. G., Stewart, D. I. & Cousens, T. W. (1998). The effects of salt solutions on the properties of bentonite–sand mixtures. *Clay Miner.* **33**, 651–660.

Tay, Y. Y. (2000). *Effect of desiccation on the performance of bentonite–sand landfill liners*. PhD thesis, University of Leeds.

Toll, D. G. (1990). A framework for unsaturated soil behaviour. *Géotechnique* **40**, No. 1, 31–44.

Wheeler, S. J. & Sivakumar, V. (1995). An elasto-plastic critical state framework for unsaturated soil. *Géotechnique* **45**, No. 1, 35–53.